

X International Conference on Structural Dynamics, EURODYN 2017

Measurements on the Vehicle-Track Interaction and the Excitation of Railway-Induced Ground Vibration

Lutz Auersch^{a*}, Samir Said^a, Roger Müller^b

^a*Federal Institute of Material Research and Testing, 12200 Berlin, Germany*

^b*Swiss Railways, Infrastructure, 3000 Bern 65, Switzerland*

Abstract

Two railway measurement campaigns have been performed in Germany and Switzerland which yield insight in the vehicle-track-soil interaction. The campaign in Germany has included simultaneous measurement of vehicle, track, and soil vibrations during train runs with 16, 25, 40, 63, 80, 100, 125, 140, 160 km/h, and impulse measurements of the passenger car, three track sections and the soil. Two ballast tracks, one on the soil surface and one on a concrete bridge, have been investigated as well as a slab track in a tunnel. Ten different sites in Switzerland have been measured for soil properties and train-induced ground vibrations, which allow to determine the excitation forces of the railway traffic. New axle-box measurements at some of the Swiss sites have been analysed to get further experimental evidence. All these measurements have been evaluated to characterize the excitation processes. Relations between vehicle vibration and ground vibration can be observed. The vehicle vibrations, namely the accelerations of the wheelsets, yield the dynamic forces due to the passage over the irregularities of the vehicle and the track. The ground vibrations are correlated to these dynamic forces to a certain extent. Some mid-frequency ground vibration amplitudes, however, are higher than expected from the dynamic excitation forces. The experimental observations can be explained by an irregular response to the passage of the static loads, that means the passage of the static loads over an irregular ballast or soil. This correct understanding of the excitation processes is important for the prediction as well as for the mitigation of railway induced ground vibrations.

© 2017 The Authors. Published by Elsevier Ltd.

Peer-review under responsibility of the organizing committee of EURODYN 2017.

Keywords: vehicle-track interaction, ground vibration, track vibration, railway measurement campaign, axle box measurements

© 2017 The Authors. Published by Elsevier Ltd.

Peer-review under responsibility of the organizing committee of EURODYN 2017.

* Corresponding author. Tel.: +49-30-81043290; fax: +49-30-81041729.

E-mail address: lutz.auersch-saworski@bam.de

1. Axle-box measurements

The Swiss Railways (SBB) have performed axle-box measurements at the sites Selzach, Pieterlen, Lengnau, Brunnen, Le Landeron (2013, IC-tilting train), and Rubigen (2012, IC-carriage EW4) [1]. The first and the last axle of the measuring car have been instrumented with an accelerometer at each axle box. The measuring train traveled with 140 to 160 km/h along the sites where BAM has measured the ground vibrations.

Some results are presented in Figure 1. The four wheels yield almost the same acceleration spectra $a(f)$ (Fig. 1a,b) except for track sections with switches where the side of the car passing the frog is clearly amplified (Fig. 1c).

Consecutive track sections show mainly the same results up to a frequency of $f = 100$ Hz (Fig. 1d,e). At site Lengnau (Fig. 1e), the axle-box spectra have nearly identical peaks at 12 and 25 Hz. These peaks could be the first and second wheel out-of-roundness (higher order out-of-roundness cannot be distinguished in the one-third octave band spectra). Finally in Figure 1f, the average amplitudes of the four wheels have been evaluated for several different sites. Even for the different sites, the differences are relatively small namely for the low frequencies between 8 and 40 Hz. The acceleration amplitudes a are usually between

$$a = 0,3 \text{ m/s}^2 \text{ and } 1 \text{ m/s}^2$$

at these low frequencies. For frequencies above $f = 40$ Hz, the amplitudes increase and reach a higher level at high frequencies. The high-frequency behavior differs for different sites. At Selzach and Brunnen a clear maximum of $a = 10 \text{ m/s}^2$ is reached at 125 Hz. The other sites have maximum amplitudes of about

$$a = 3 \text{ m/s}^2.$$

At Lengnau (Fig. 1e) the high-frequency spectra vary due to different under sleeper pads at different track sections.

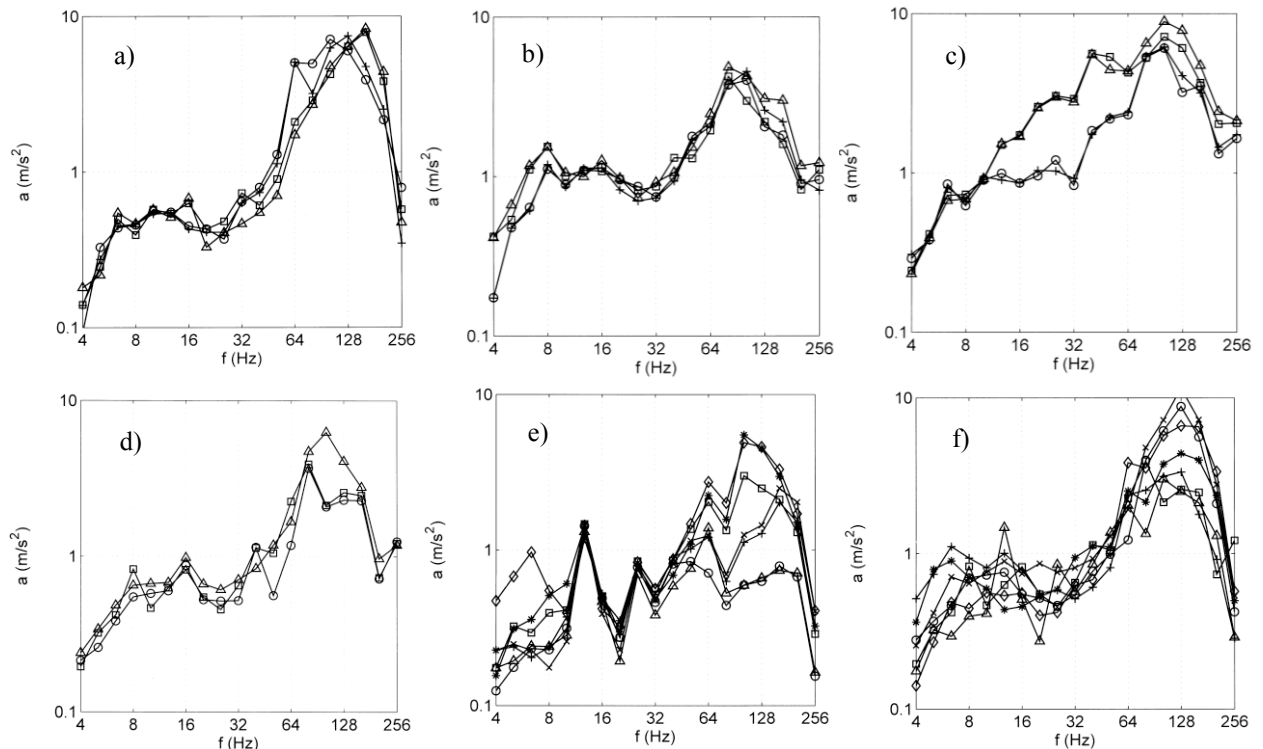


Fig. 1. Axle-box accelerations a as a function of frequency f (a) of four wheels at Le Landeron; (b) at Rubigen; (c) at Rubigen with switch; (d) of three track sections at Rubigen; (e) of seven track sections in Lengnau; (f) of the sites \square Rubigen, \circ Selzach, \triangle Lengnau, $+$ Pieterlen, \times Brunnen, \diamond Le Landeron N, $*$ Le Landeron S, (Figs d, e, f average of 4 wheels).

In the BAM research project „vehicle-track interaction“ [2], axle-box measurements had been performed by German Railways (DB) 1994 at measuring site Wiesenfeld on the high-speed line near Würzburg. The train run with specified speeds of 40, 63, 80, 100, 120, 140, 160 km/h over different track situations. Figure 2a and 2b show the

results for two of the four measured wheels when running over a ballast track. Figure 2c shows the corresponding results of a slab track. The results of the ballast track for $v_T = 160$ km/h are very similar to the measurements in Switzerland. The lower amplitude level at low frequencies and the higher amplitudes at high frequencies are confirmed.

The influence of the train speed on the low frequencies is very regular, the amplitudes increase as $A \sim v_T^2$ and are shifted to higher frequencies proportional to the train speed v_T . At higher frequencies, the shift of dominant frequencies, for example the sleeper-distance frequency can be observed in Figure 2a. Other characteristics stay constant in frequency and amplitude. The high frequency range includes the vehicle-track resonance which is at 80 to 100 Hz for the ballast track and at 64 Hz for the slab track in Figure 2c. The resonance of the slab track at 64 Hz is clearer, it has a higher amplification and a sharper resonance region. The ballast track has a stronger radiation damping into the soil which yields a smoother resonance curve [3].

Below the resonance frequency, the wheelset follows directly the irregularities s of the vehicle-track-soil system. Around and above the resonance frequency, the irregularities are amplified or reduced by the wheelset mass. At the Wiesenfeld site, the soil is quite stiff and the vehicle-track-soil resonance is quite high. Therefore, the displacement amplitudes s of the irregularities can be determined from the axle-box accelerations in a wide frequency range. The irregularities are highest at low frequencies and decrease with $s \sim f^{-2}$. The amplitudes are between $s(16$ Hz, 160 km/h) = 0.03 and 0.1 mm [4]. At low frequencies, the track and soil irregularities are dominating whereas the wheel and rail roughness are the main excitation at high frequencies where the wheelset responses are modified by the vehicle-track interaction.

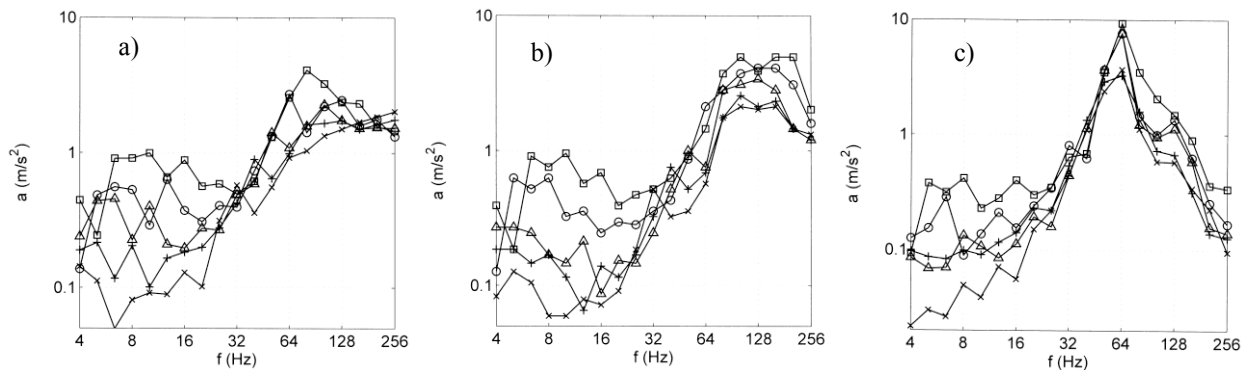


Fig. 2. Axle-box accelerations a as a function of frequency f (a) of wheel 1; (b) of wheel 2 on a ballast track; (c) on a slab track in a tunnel at Wiesenfeld; variation of the train speed \square 160, \circ 125, \triangle 100, $+$ 80, \times 63 km/h.

2. Ground vibration measurements

BAM has performed ground vibration measurements at 11 sites near railway lines in Switzerland [5]. The train induced ground vibrations have been measured, but also the wave propagation due to hammer impacts. It could be concluded from the impact measurements that all these sites consist of a layer on a stiffer half-space, but with site-specific stiffnesses of the layers and the half-spaces [6]. Figure 3 shows the train induced ground vibration velocities v at 6 of the 11 sites. The one-third octave band spectra comprise four decades of amplitudes where the strong differences can be found for the different distances from 4 to 60 m and for the different frequencies. At low frequencies, very low amplitudes occur because the particle velocities start with zero amplitude at zero frequency, but also because of the stiff underlying half-space. The amplitudes increase rapidly with frequency, at some sites over the whole frequency range (Fig. 3a-c). At some other sites (Fig. 3d-f), the amplitude curves turn to horizontals above a site-specific mid frequency. Generally for all sites, the high-frequency amplitudes are very different for different distances indicating a strong attenuation with distance which is attributed to the material damping of the soil [7]. The inferior attenuation at low and mid frequencies is due to the missing damping effect, see also Section 4.

3. Prediction of ground vibration for different homogeneous or layered soil models and back-calculation

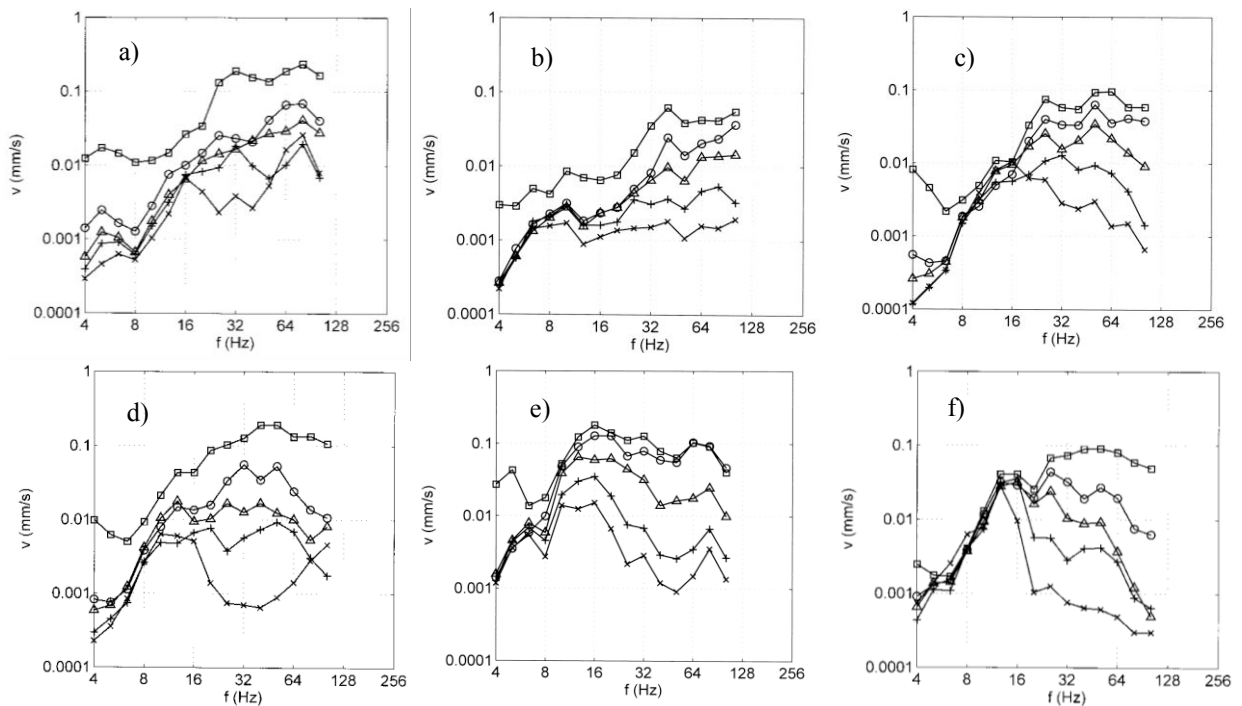


Fig. 3. Train induced ground vibration velocities v as a function of frequency f at the measuring sites (a) Rubigen; (b) Dottikon; (c) Hindelbank; (d) Brunnen; (e) Selzach; (f) Lengnau; distances $r \approx \square, \circ, \triangle, +, \times$ 4, 8, 16, 32, 64 m.

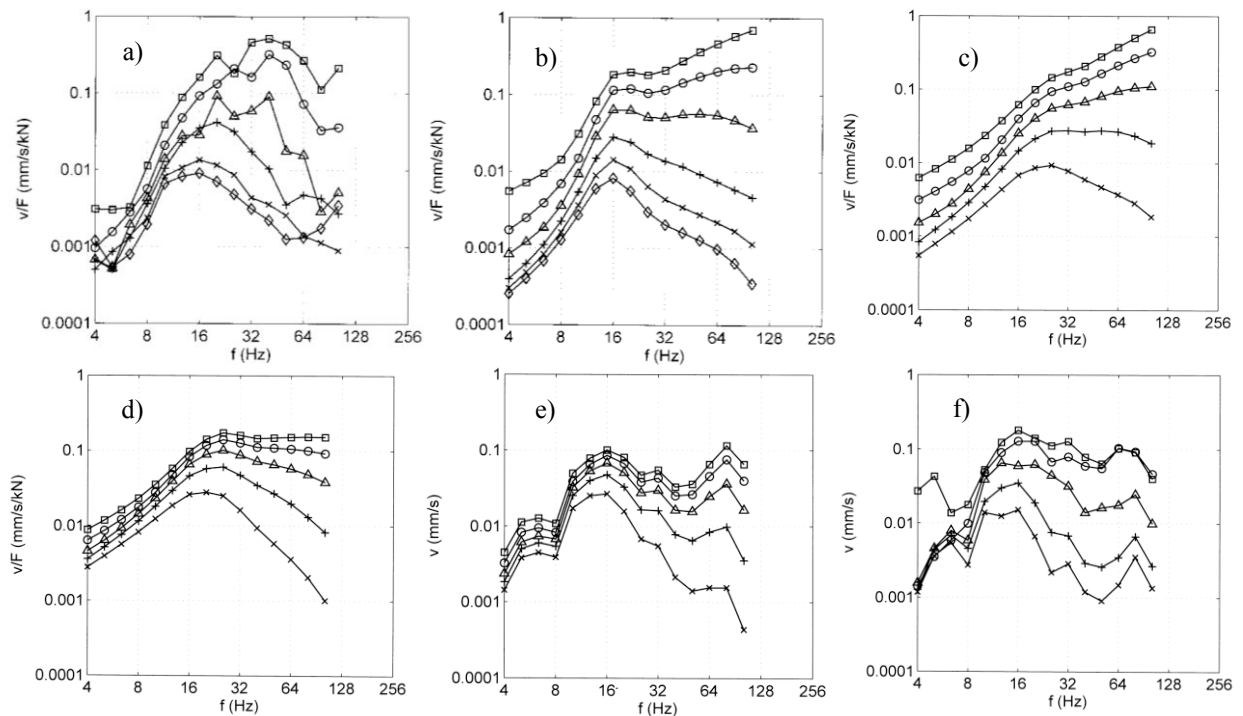


Fig. 4. Ground vibration velocities $v(f)$ and transfer functions $v/F(f)$ at Selzach (a) hammer impact; (b) approximated transfer function point-load; (c) transfer function from wave dispersion measurements; (d) transfer function for train load; (e) predicted train-induced ground vibration; (f) measured train-induced ground vibration; distances $r \approx \square, \circ, \triangle, +, \times$ 4, 8, 16, 32, 64 m.

The wave propagation measurements are evaluated either for the frequency-dependent wave velocity (dispersion) or for the transfer function (of a point load, the hammer excitation Fig. 4a, [5, 6]). Many layered soil models are calculated and the best fit either to the dispersion curve (Fig. 4c) or to the transfer function (Fig. 4b) is used for the further calculation. Note that both approximations differ only in details whereas low- and high-frequency levels are almost the same. The point-load transfer function can be superposed to get the transfer function of a train (Fig. 4d). Finally, the force spectrum $F(f)$ is calculated which yields the best approximation (Fig. 4e) of the measured train-induced ground vibration (Fig. 4f). The observation, that the predicted (Fig. 4e) or measured (Fig. 4f) train vibrations are quite similar to the transfer functions (Fig. 4d), has been found for most of the train measurements in Figure 3 so that they represent well the characteristics of the different sites. Figures 3a,b,c represent a dominating stiff soil whereas a thicker soft top layer is characteristic in Figures 3 d,e,f. Figure 5 demonstrates the similar procedure for the German site Wiesenfeld (1994), the transfer function from hammer impact (Fig. 5a), the transfer function for train load (Fig. 5b), and the measured train-induced vibration (Fig. 5c) which incorporates a similar strong mid-frequency component as at the Swiss site Lengnau in Figure 3f.

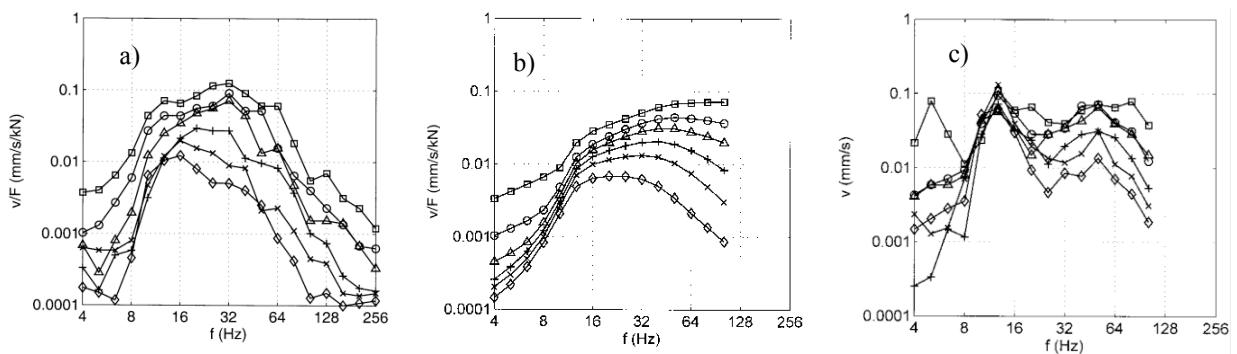


Fig. 5. Ground vibration velocities $v(f)$ and transfer functions $v/F(f)$ at Wiesenfeld (a) hammer impact; (b) approximated transfer function for train load; (c) measured train-induced ground vibration; distances $r \approx \square 3, \circ 5, \triangle 10, + 20, \times 30, \diamond 50$ m.

4. Dynamic axle loads (force spectra)

The force spectra which have been back-calculated from the train induced ground vibrations are presented in Figure 6a,b for all measuring sites in Switzerland and some additional sites in Germany. The force amplitudes are around 1 kN for all frequencies, mostly between 0.3 and 3.0 kN.

The axle-box measurements can also be evaluated for the dynamic axle loads. Under the assumption of a rigid wheelset, which is certainly true for the low frequency range, the forces F are calculated as

$$F = m_R a$$

with a wheelset mass of $m_R = 1500$ kg and the axle-box acceleration a . The axle-box results for the same sites as in Figure 6a are presented in Figure 6c. At the low frequencies, the dynamic axle loads are around 1 kN in good agreement with the ground vibration results. The high-frequency forces are higher in the range of 1 to 10 kN. This cannot be found in the forces from ground vibration measurements. The discrepancy can be due to the possible flexible behavior of the wheelset [8] and due to the strong damping effects of the soil [7].

(In addition, the axle-box accelerations and the ground vibrations have also been analysed for several switches [5]. The same influence of the switch has been found for both measurements, an amplification in the whole frequency range with a maximum around 40 Hz.)

Besides the big difference at high frequencies, there are minor low-frequency differences at some of the sites with normal tracks. In the frequency range between 8 and 20 Hz (or specially between 10 and 16 Hz), the force amplitudes reach values of 8 kN at the sites Lengnau and Wiesenfeld (Fig. 6a). The same mid-frequency range is amplified at three other German sites and two more Swiss sites (Fig. 6b) also show an amplification. These higher amplitudes cannot be generated by the inertial forces of the wheelset. A possible reason is the scattering of the impulse load from the passage of the static axle loads if the train is running on a soil with randomly varying stiffness [9]. The weak attenuation of the ground amplitudes (Figs. 3f, 5c) also points to the scattered axle impulses.

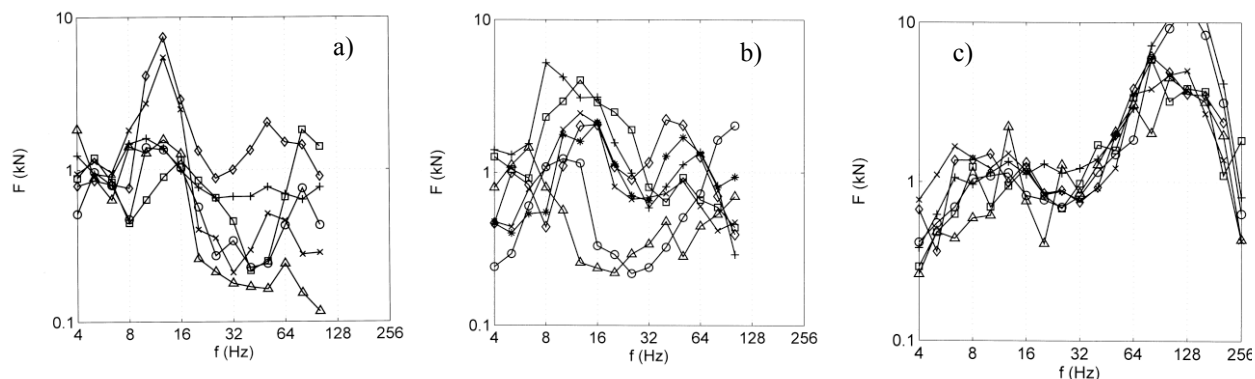


Fig. 6. Dynamic axle load spectra $F(f)$ from ground vibration measurements (a) sites with additional axle-box measurements \square Rubigen, \circ Selzach, \triangle Pieterlen, $+$ Brunnen, \times Lengnau, \diamond Wiesenfeld; (b) additional sites \square Hindelbank, \circ Hausen, \triangle Dottikon, $+$ Berg, \times Altheim, \diamond Waghäusel, $*$ Hirschaid, and (c) from axle-box-measurements at the sites \square Rubigen, \circ Selzach, \triangle Lengnau, $+$ Pieterlen, \times Brunnen, \diamond Le Landeron.

5. Conclusion

The coupling of axle-box measurements and ground vibration measurements has been shown as a very useful method to analyse the excitation of train-induced ground vibration. In cooperation of BAM and SBB several Swiss sites could be analysed. The transfer functions for the wave propagation at these sites have been determined from hammer tests and used to determine the dynamic axle-load spectra. These spectra are compared with the axle-load spectra from the axle-box measurements showing generally the correct force level (1 kN per axle and one-third octave). Arguments have been given for the higher high-frequency forces from the axle-box measurements, and especially for a certain low-frequency range where the higher ground vibration amplitudes may be generated by an irregular soil at some of the sites. Generally, the comparison of axle-box and ground measurements confirm the prediction of train induced ground vibration by continuum mechanical models.

Acknowledgements

The measurements at the Swiss sites have been performed by W. Wuttke, S. Said, F. Ziegler, and W. Schmid.

References

- [1] P. Dutoit: Intercity-Neigezug und Reisezugwagen, Spezialmessung vertikale Beschleunigungen an Achsbüchsen. Bericht, SBB, Bern, 2016.
- [2] L. Auersch, S. Said, W. Rücker, Das Fahrzeug-Fahrweg-Verhalten und die Umgebungserschütterungen bei Eisenbahnen, BAM-Forschungsbericht 243, Berlin, 2001.
- [3] L. Auersch, The excitation of ground vibration by rail traffic: Theory of vehicle-track-soil interaction and measurements on high-speed lines. *Journal of Sound and Vibration* 284, (2005) 103-132.
- [4] L. Auersch, Theoretical and experimental excitation force spectra for railway induced ground vibration – vehicle-track soil interaction, irregularities and soil measurements. *Vehicle System Dynamics* 48 (2010) 235 – 261.
- [5] L. Auersch, S. Said: Einfluss der Bodenparameter und von Weichen auf die Erschütterungsemission von Zügen. Bericht für die Schweizerischen Bundesbahnen, BAM, Berlin, 2014.
- [6] L. Auersch, S. Said, Comparison of different dispersion evaluation methods and a case history with the inversion to a soil model, related admittance functions, and the prediction of train induced ground vibration, *Journal of Near Surface Geophysics* 13 (2015) 127-142.
- [7] L. Auersch, Technically induced surface wave fields, Part II: Measured and calculated admittance spectra, *Bulletin of the Seismological Society of America* 100 (2010) 1540-1550.
- [8] L. Auersch, Vehicle dynamics and dynamic excitation forces of railway induced ground vibration, *Proceedings of the 21st International Symposium on Dynamics of Vehicles on Roads and Tracks, KTH Stockholm, 2009, (CD-ROM), pp. 1-12.*
- [9] L. Auersch, Ground vibration due to railway traffic – The calculation of the effects of moving static loads and their experimental verification. *Journal of Sound and Vibration* 293 (2006) 599-610.
- [10] G. Müller, M. Möser (eds), *Handbook of Engineering Acoustics*. Springer, Berlin Heidelberg, 2014.
- [11] D. Thompson, *Railway noise and vibration*. Elsevier Science, Amsterdam, 2008.